VERTICAL OSCILLATION OF EARTH AND ROCKFILL DAMS: ANALYSIS AND FIELD OBSERVATION

GEORGE GAZETAS*

ABSTRACT

Although vertical oscillations may have a profound effect on the seismic stability and deformability of embankment dams, they have received so far little, if any, attention. Filling this gap, the paper develops a simple but realistic two-dimensional method for evaluating the dynamic characteristics and analyzing the seismic behaviour of earth and rockfill dams oscillating in the vertical direction. Shear and dilatational deformations are considered, the dependence of soil stiffness on confining pressure is rationally modeled and the effect of canyon geometry is approximately treated. Numerical results are portrayed in the form of dimensionless graphs of natural frequencies, modal displacement shapes and modal participation factors as functions of characteristic geometric and material parameters. To demonstrate the capability of the developed model to successfully predict the field performance of actual dams, three case studies are presented involving two earth and one rockfill dam from three seismically active countries. Reasonably good agreement is obtained between computed and observed (during earthquake shaking) natural frequencies and vertical crest accelerations.

Key words: dam, dynamic, earthfill, earthquake, heterogeneity, rockfill, vertical load
IGC: E 8/C 7/G 6

INTRODUCTION

Significant progress has been made in recent years towards understanding the behaviour of earth and rockfill dams subjected to earthquake shaking. However, the developed analytical procedures for evaluating the seismic stability and potential deformations of such dams consider only horizontal ground excitation, either in the upstream–downstream (i.e. lateral) or in the longitudinal direction (e.g., Hatanaka, 1955; Ambraseys, 1960; Ishizaki et al., 1962; Chopra, 1967; Minami, 1969; Makdisi et al., 1978; Seed, 1979; Mori et al., 1980; Gazetas, 1981 a, b; Abdel-Ghaffar et al., 1981). Yet, there is ample evidence of substantial vertical oscillations of embankment dams, arising from the vertical component of earthquake ground motions. For example, Fig. 1 portrays the vertical components of acceleration, velocity and displacement time histories recorded at the crest of the Infiernillo Dam, in Mexico, during a magnitude 7.6 earthquake which occurred at an epicentral distance of about 87 km on March 14, 1979 (Comisión Federal de Electricidad, 1980). The relatively high intensity (e.g., peak acceleration of about 340 gal) and long duration of the motion are evident.

* Associate Professor of Civil Engineering, Rensselaer Polytechnic Institute, Troy, New York, 12181, USA ; formely Assistant Professor of Civil Engineering, Case Western Reserve University, Cleveland, Ohio, USA.
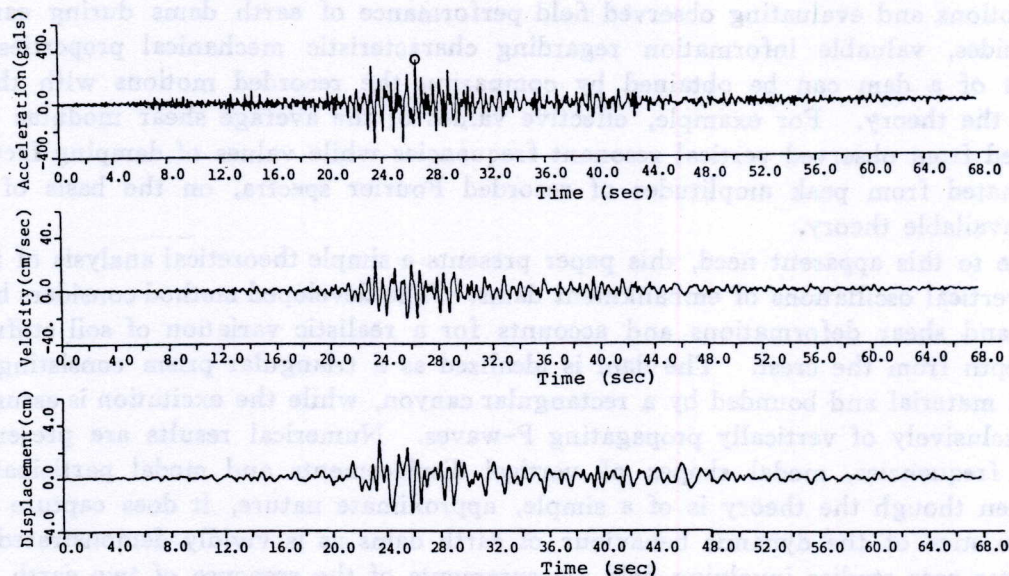
Fig. 1. Vertical component of motion at center of crest of El Infiernillo Dam in Mexico, during the March 14, 1979 earthquake (Comisión Federal Electricidad, (1980))

It is widely believed that lateral and longitudinal vibrations are solely responsible for the most frequently observed types of serious damage in embankment dams, namely: longitudinal cracking near the crest center, sliding of soil masses from the upstream or downstream slopes, transverse cracking near the crest edges and large permanent displacements or bearing capacity failures due to liquefaction of saturated cohesionless soils in the dam. Nevertheless, there can be little doubt that strong vertical oscillations may have a profound effect on the seismic stability and deformability of embankment dams. For instance, the residual displacements of a potentially sliding mass, the generation of pore-water pressures and development of large strains in zones of cohesionless soil, and the potential loss of strength of clayey soils depend to a considerable extent on vertical accelerations and vertical dynamic stresses, as schematically illustrated in Fig. 2. Therefore, the development of an analytical method for computing the response of earth and rockfill dams to vertical ground shaking is greatly warranted.

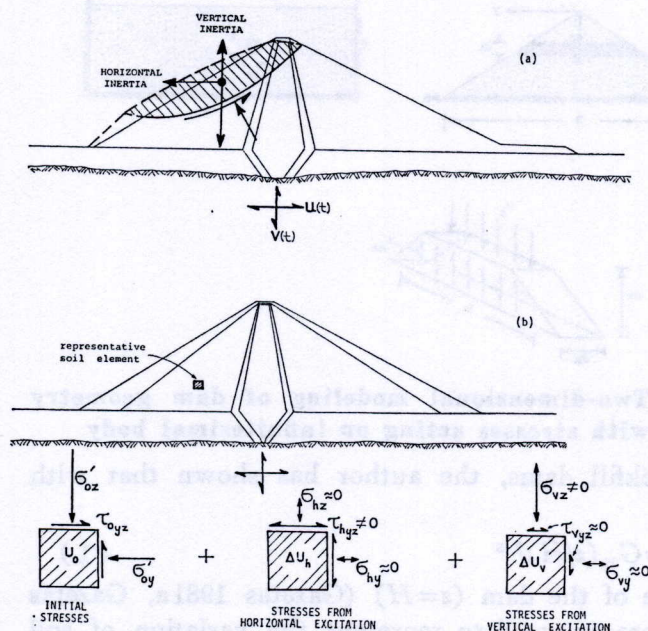It should also be noted that a vertical vibration theory may be a useful tool in interpreting recorded

Fig. 2. Schematic illustration of effects of vertical oscillations of a dam:
(a) on stability and permanent displacements of a potential slide mass
(b) on generation of pore-water pressures that may lead to liquefaction of saturated cohesionless soils

(vertical) motions and evaluating observed field performance of earth dams during earth-quakes. Besides, valuable information regarding characteristic mechanical properties of the materials of a dam can be obtained by comparing the recorded motions with those predicted by the theory. For example, effective values of the average shear modulus can be backfigured from observed vertical resonant frequencies while values of damping factors can be estimated from peak amplitudes of recorded Fourier spectra, on the basis of an appropriate available theory.

In response to this apparent need, this paper presents a simple theoretical analysis of free and forced vertical oscillations of embankment dams. The developed method considers both dilatational and shear deformations and accounts for a realistic variation of soil stiffness along the depth from the crest. The dam is idealized as a triangular prism consisting of linear elastic material and bounded by a rectangular canyon, while the excitation is assumed to consist exclusively of vertically propagating P-waves. Numerical results are presented for natural frequencies, modal shapes of vertical displacements and modal participation factors. Even though the theory is of a simple, approximate nature, it does capture the key characteristics of the dynamic behaviour of earth dams as is vividly demonstrated by means of three case studies involving field measurements of the response of two earth and one rockfill dam during actual earthquakes.

FREE VIBRATION ANALYSIS

Simplifying Assumptions

With reference to the system of coordinate axes shown in Fig. 3, the following simplifying assumptions are made in order to derive the governing equations of motion:

1. The dam consists of uniform material having a constant mass density, ρ, and a constant Poisson's ratio, ν, but variable elastic moduli in shear and compression, G and E, reflecting the dependence of soil stiffness on effective normal octahedral stress. On the basis of theoretical (finite element) analyses, results of experimental testing and geophysical

Fig. 3. Two-dimensional modeling of dam geometry with stresses acting on infinitesimal body

measurements on many actual earth and rockfill dams, the author has shown that with very good accuracy

$$G = G(z) = G_m (z/H)^{2/3} \qquad (1)$$

where G_m = maximum value of G at the base of the dam ($z=H$) (Gazetas 1981a, Gazetas & Abdel-Ghaffar, 1981). Eq. (1) is therefore assumed to represent the variation of soil stiffness with depth from the crest.

2. The soil exhibits linear stress-strain behaviour–an assumption which is acceptable for small levels of strain but contradicts reality at strains larger than about 0.01 percent. Note, however, that in practice this is often overcome by performing a series of linear analyses using soil moduli and damping factors consistent with the level of strains resulting from the previous analysis ('*strain compatible viscoelastic model*'). See, e.g., Makdisi et
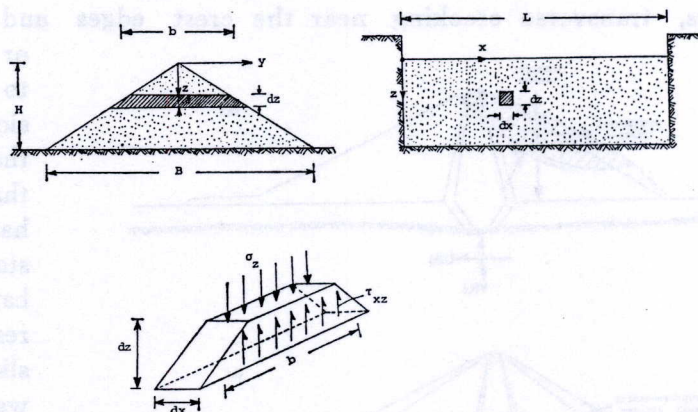
al., 1978; Richart et al., 1977; Mori et al., 1980.

3. The normal and shear stresses, σ_z and τ_{xz}, are independent of y and, thus, uniformly distributed over infinitesimal areas $b \cdot dx$ and $b \cdot dz$ respectively. This simplifying assumption is similar to the hypothesis of uniform shear stresses τ_{zy} over areas $b \cdot dx$ that forms the basis of the shear-beam theory of lateral vibrations (Okamoto, 1973). Plane-strain finite element analyses clearly confirm the present hypothesis as a reasonable simplification of reality: except for a small area near the faces of the dam, σ_z and τ_{xz} are almost uniform across the width of a dam, i.e. along the y axis.

4. The vertical displacement, v, is also independent of y and no horizontal longitudinal deformations occur. These assumptions, although of simplifying approximate nature, respect the boundary conditions of the problem and are consistent with the hypotheses of the preceding section 3.

5. The reservoir water has a negligible influence on the response of the dam.

Governing Equations

Denoting by $v(x, z; t)$ the vertical motion relative to the boundaries, one may express the net normal and shearing forces on an infinitesimal element of the dam of volume $b \cdot dx \cdot dz = (B/H) \cdot z \cdot dx \cdot dz$ as

$$-\frac{B}{H} \frac{\partial}{\partial z} [z \cdot \sigma_z(x, z; t)] \cdot dx \cdot dz \tag{2a}$$

and

$$-\frac{B}{H} \frac{\partial}{\partial x} [\tau_{xz}(x, z; t)] \cdot z \cdot dx \cdot dz \tag{2b}$$

respectively, while the inertia force is given by

$$\rho \cdot \ddot{v}(x, z; t) \cdot \frac{B}{H} \cdot z \cdot dx \cdot dz \tag{2c}$$

Equating the sum of the three forces to zero leads to

$$\eta \rho \ddot{v} = \frac{1}{z} \frac{\partial}{\partial z} \left[G(z) \cdot z \cdot \frac{\partial v}{\partial z} \right] + \eta G(z) \cdot \frac{\partial^2 v}{\partial x^2} \tag{3}$$

after making use of the following stress-displacement relations, which are consistent with assumptions 3 and 4:

$$\tau_{xz} = G(z) \frac{\partial v}{\partial x} \tag{4a}$$

$$\sigma_z = \frac{E(z)}{1 - \nu^2} \frac{\partial v}{\partial z} = \frac{G(z)}{\eta} \frac{\partial v}{\partial z} \tag{4b}*$$

where

$$\eta = (1 - \nu)/2 \tag{4c}$$

The appropriate boundary conditions that should be respected by a physically meaningful solution of Eq. (3) are

$$v(0, z; t) = v(L, z; t) = v(x, H; t) = 0 \tag{5a}$$

$$\sigma_z(x, 0; t) = 0 \tag{5b}$$

that is, no separation is allowed between the freely oscillating dam and the stationary supporting canyon and no normal tractions should arise at the crest.

Solution

The solution of Eq. (3) with $G(z)$ varying according to Eq. (1) can be cast in the form

---

* This relation was derived on the basis of the elastic constitutive relations by assuming vanishing longitudinal strains ($\varepsilon_x = 0$) and vanishing lateral confining pressure ($\sigma_y = 0$).

$$v(x, z ; t) = V(x, z) \cdot \exp(i\omega t) \tag{6a}$$

where

$$V(x, z) = N(x) \cdot M(z) \tag{6b}$$

and ω represents the circular frequency of vibration ($i = \sqrt{-1}$). Eqs. (6), (3) and (1) lead after some algebra to

$$\frac{1}{M}\frac{d^2M}{dz^2} + \frac{5}{3}\frac{1}{zM}\frac{dM}{dz} + k^2\left(\frac{H}{z}\right)^{2/3} = -\eta\frac{1}{N}\frac{d^2N}{dx^2} \tag{7}$$

in which $k^2 = \eta\rho\omega^2/G_m$. Since the left side of Eq. (7) is a function of z only, whereas the right side is a function of x only, Eq. (7) implies that both sides attain c constant value independent of x and z. Denoting this constant by ηa^2 one obtains from the right side:

$$\frac{d^2N}{dx^2} + a^2N = 0 \tag{8}$$

The solution of Eq. (8) that satisfied (5a) is

$$N(x) = N_r(x/L) = A' \sin a_r x; \quad a_r = r\pi/L, \quad r = 1, 2, 3, \cdots \tag{9}$$

in which A' is an indeterminate constant. The left side of Eq. (7) yields

$$u^2\frac{d^2M}{du^2} + 2u\frac{dM}{du} + \frac{9}{4}u^2(k^2H^{2/3} - \eta a_r^2 u)M = 0 \tag{10}$$

where, for mathematical convenience, the following transformation of the dependent variable has been introduced

$$z = u^{3/2} \tag{11}$$

Equations similar in form with Eq. (10) have been recently considered by Abdel–Ghaffar and Koh (1981) who utilized the Frobenius method to obtain solutions expressed as (convergent) power series of u, of the form

$$M(u) = \sum_{j=0}^{\infty} b_j u^{j+s} \tag{12}$$

Applying the technique to Eq. (10), while accounting for Eq. (11) and the boundary conditions [Eqs. (5)], furnishes

$$M(z) = M_{nr}(z/H)$$
$$= A''\left[1 - \frac{9/4}{2\cdot3}\Omega_{nr}^2\left(\frac{z}{H}\right)^{4/3} + \frac{9/4}{3\cdot4}\eta\alpha_r^2\left(\frac{z}{H}\right)^{6/3} + \cdots\right] \tag{13}$$
$$n, r = 1, 2, 3, \cdots$$

in which

$$\Omega_{nr} = k_{nr}H = \omega_{nr}\sqrt{\eta}\,\frac{H}{C_m}; \quad C_m = \left(\frac{G_m}{\rho}\right)^{1/2} \tag{14a}$$

are the roots of

$$M_{nr}(1) = 0 \tag{14b}*$$

and

$$\alpha_r = a_r H = r\pi H/L, \quad r = 1, 2, 3, \cdots \tag{15}$$

It is evident from Eqs. (13)–(14) that Ω_{nr} is a function of $\eta\alpha_r^2$ only. The first five roots of Eq. (14b), that is the values Ω_{1r}, Ω_{2r}, Ω_{3r}, Ω_{4r} and Ω_{5r}, have been numerically evaluated and are plotted in Fig. 4 versus $\eta\alpha_r^2$. Given the geometry and Poisson's ratio

---

* Notice that Eq. (14b) enforces the boundary restriction of vanishing displacements at $z = H$, i. e.,
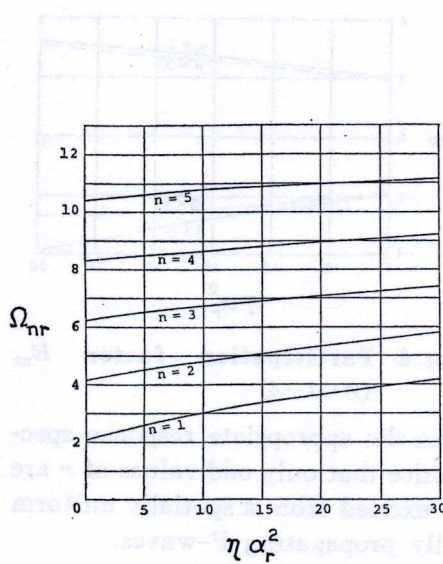$v(x, H; t) = 0$

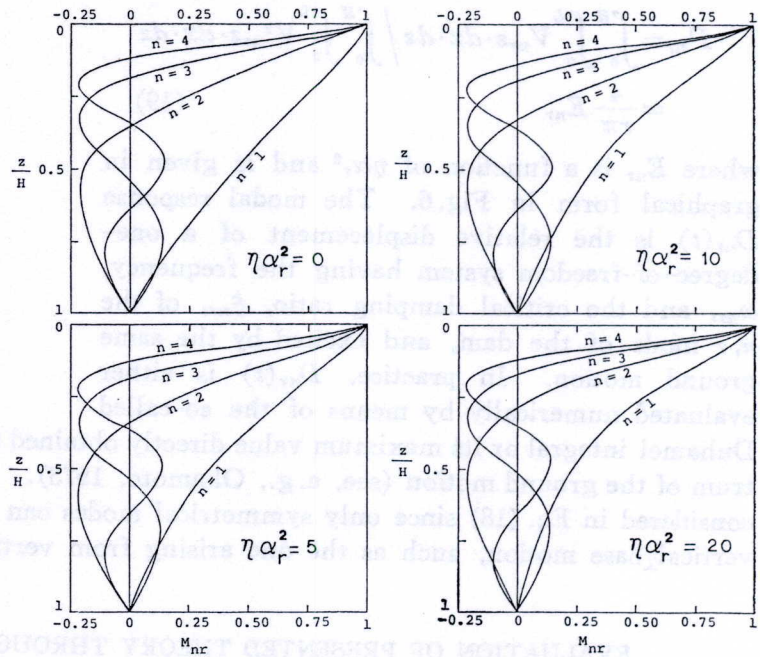Fig. 4. **Normalized frequency factor Ω_{nr} ($n=1-5$)**

Fig. 5. **Modal vertical displacement shapes in the z-direction for different values of the $\eta\,\alpha_r^2$ factor ($n=1-4$)**

of a dam, the value $\eta\alpha_r^2=\dfrac{1-\nu}{2}\left(\dfrac{\pi r H}{L}\right)^2$ can be computed for each modal-wave form number r, along the x axis; then the Ω_{nr} values are read from Fig. 4 for each modal wave form number n, along the z axis, and the natural frequencies ω_{nr} are calculated from Eq. (14a). The displacement shapes, normalized to a unit peak amplitude, are

$$V_{nr}=M_{nr}(z/H)\cdot\sin\left(r\pi\,\frac{x}{L}\right) \qquad (16)$$
$$n,r=1,2,3,\cdots$$

where the modal shapes in the z-direction, M_{nr}, computed from Eq. (13) for four different values of the dimensionless parameter $\eta\;\alpha_r^2$ and $n=1-4$, are graphically displayed in Fig. 5. Since the range of values of the dimensionless parameter (from 0 to 20) covers a wide class of embankment dams, Fig. 5 (along with Fig. 4) can be readily used in practice to evaluate modal displacements and frequencies without a need to resort into numerical computation from Eqs. (13) and (14).

ANALYSIS OF SEISMIC RESPONSE

Since, as it can be easily shown, the mode shapes V_{nr} satisfy the orthogonality condition

$$\int_0^H\int_0^L\left(\rho\,\frac{B}{H}\,zdxdz\,V_{nr}V_{mq}\right)=0 \quad n\neq m,\quad r\neq q \qquad (17)$$

modal superposition can be used to compute the response of a dam to external excitation. During earthquake shaking that consists exclusively of vertically propagating dilatational waves the vertical displacements of the dam relative to the surrounding canyon are

$$v(x,z\,;t)=\sum_{n=1,2,\cdots}^{\infty}\sum_{r=1,3,5,\cdots}^{\infty}\Gamma_{nr}\cdot V_{nr}(x,z)\cdot D_{nr}(t) \qquad (18)$$

in which Γ_{nr} is the modal participation factor of the n,r mode:

$$\Gamma_{nr} = \int_0^H \int_0^L V_{nr} z \cdot dx \cdot dz \bigg/ \int_0^H \int_0^L V^2_{nr} z \cdot dx \cdot dz$$

$$= \frac{4}{r\pi} E_{nr} \tag{19}$$

where E_{nr} is a function of $\eta \alpha_r^2$ and is given in graphical form in Fig. 6. The modal response $D_{nr}(t)$ is the relative displacement of a one-degree-of-freedom system having the frequency, ω_{nr}, and the critical damping ratio, ξ_{nr}, of the n, r mode of the dam, and excited by the same ground motion. In practice, $D_{nr}(t)$ is either evaluated numerically by means of the so-called Duhamel integral or its maximum value directly obtained from the appropriate response spectrum of the ground motion (see, e.g., Okamoto, 1973). Notice that only odd values of r are considered in Eq. (18) since only symmetrical modes can be excited from a spatially uniform vertical base motion, such as the one arising from vertically propagating P-waves.
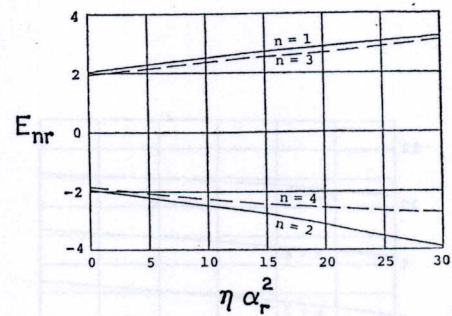
Fig. 6 Participation factor E_{nr}
$(n=1-4)$

EVALUATION OF PRESENTED THEORY THROUGH FIELD MEASUREMENTS

A simplified analysis procedure, like the one presented in this paper, can only serve as a useful tool in the seismic design if it successfully interprets phenomena observed on appropriately instrumented earth or rockfill dams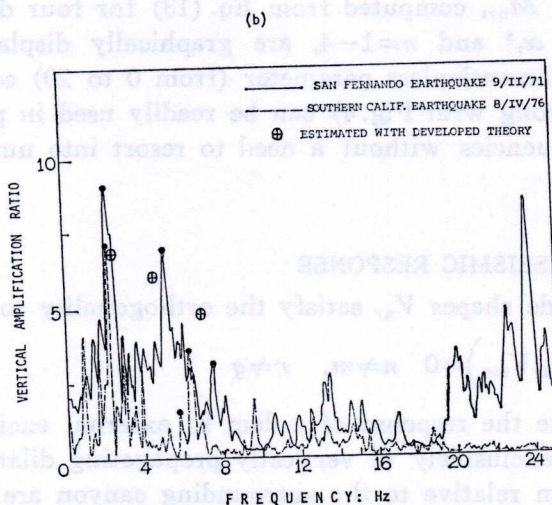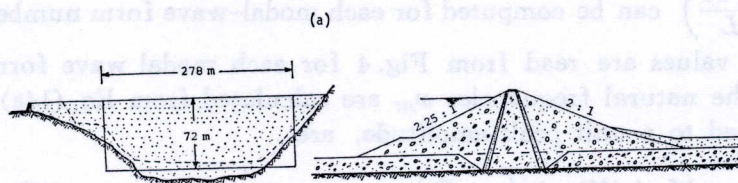 during actual earthquakes. In other words, confidence in using the method cannot be gained unless it is demonstrated that it does have the capability of predicting the recorded field performance of dams.

This section attempts a first evaluation of the herein developed simple theory of vertical vibrations, by utilizing earthquake records from three earth/rockfill dams located in three, different, seismically active areas (California, Mexico and Japan). It should be pointed out, moreover, that such an evaluation is useful in its own right, as it provides insight on, and perhaps understanding of, the dynamic behaviour and anticipated performance of actual dams.

Santa Felicia Earth Dam, California

The largest cross-section and a longitudinal section of

Fig. 7. (a) Geometry of Santa Felicia dam in California
(b) Crest-to-abutment amplification spectra from two earthquakes; comparison with three computed values

the dam are displayed in Fig. 7(a). The dam is a rolled–fill embankment with a central impervious core and pervious shells. Core and shell material is mostly alluvial, consisting of clay, sand, gravel and boulders. More detailed information on material properties, geometry, and so on, of the dam can be found in Abdel–Ghaffar and Scott, 1978.

On February 9, 1971, and on April 8, 1976, Santa Felicia was subjected to strong ground shaking triggered by the San Fernando (magnitude 6.5) and the Southern California (magnitude 5) earthquakes, which occurred at epicentral distances 33 km and 14 km, respectively. Maximum accelerations at the crest of the dam reached about 210 gal and 50 gal, respectively, during the two events. Analysis of the horizontal (lateral and longitudinal) records have already been published by Abdel–Ghaffar and Scott, 1978, Gazetas, 1981 b, and Abdel–Ghaffar and Koh, 1981.

Fig. 7(b) portrays the vertical amplification spectra, i.e., the ratios of Fourier spectra computed from the two pairs of vertical components of motion that were recorded at the middle of the crest and the right abutment during the two earthquakes. These spectra provide indication of the natural frequencies as well as a qualitative picture of the degree to which various natural modes participate in the shaking. The developed analytical method is used to compute the first three natural frequencies, as well as to obtain a rough estimate of the corresponding amplification ratios.

On the basis of geophysical and experimental measurements and the results of full–scale tests (Abdel–Ghaffar & Scott, 1978) it was concluded the average shear–wave velocity, C_a, of the dam lies between approximately 220 m/s and 270 m/s, for the level of shearing strains induced by the two earthquakes. Poisson's ratio was estimated to be close to 0.45. An "equivalent" dam in a rectangular canyon with $L \simeq 278$ m and $H \simeq 72$ m shown in Fig. 7(a) is chosen to approximate the actual geometry. For a velocity $C_a = 220$ m/s, the maximum velocity at the base of the dam is*

$$C_m = \frac{7}{6} C_a \simeq 256.7 \text{ m/s} \qquad (20)$$

while the normalized factor

$$\eta \alpha_r^2 = \frac{1-0.45}{2} \pi^2 (72/278)^2 \simeq 0.182$$

for $r=1$ [Eq. (15)]. The values of $\Omega_{n1}, n=1, 2, \cdots, 5$, can be read off Fig. 4. For example, $\Omega_{11} \simeq 2.10$, $\Omega_{21} \simeq 4.20$ and $\Omega_{31} \simeq 6.30$. The corresponding natural circular frequencies are then obtained from Eq. (14a).

$$\omega_{11} = \frac{\Omega_{11}}{\sqrt{\eta}} \frac{C_m}{H} \simeq \frac{2.10}{0.524} \times \frac{256.7}{72} \qquad (21)$$
$$\simeq 14.28 \text{ rad/s}$$

and, similarly, $\omega_{21} \simeq 28.56$ rad/s and $\omega_{31} \simeq 42.86$ rad/s. Or, $f_{11} \simeq 2.27$ Hz, $f_{21} \simeq 4.54$ Hz and $f_{31} \simeq 6.82$ Hz. It is readily seen that these frequencies agree very closely with the frequencies of three large peaks observed in both amplification–ratio spectra (Fig. 7(b)). Notice in particular that the 'predominant' frequencies of the two spectra (2.20 Hz for the San Fernando and 2.25 Hz for the Southern California earthquake) are only slightly smaller than the computed $f_{11} \simeq 2.27$ Hz.

Crude estimates of the amplification ratios at each of the above three frequencies have also been obtained by approximating Eq. (18) with a single term and utilizing the acceleration time history of each base motion. The average computed values for the three frequencies are depicted in Fig. 7(b) for comparison with the recorded amplification–ratios. The

* The relation between C_m and C_a is obtained by integration over the dam cross–section, using Eq. 1 (Gazetas, 1981c).
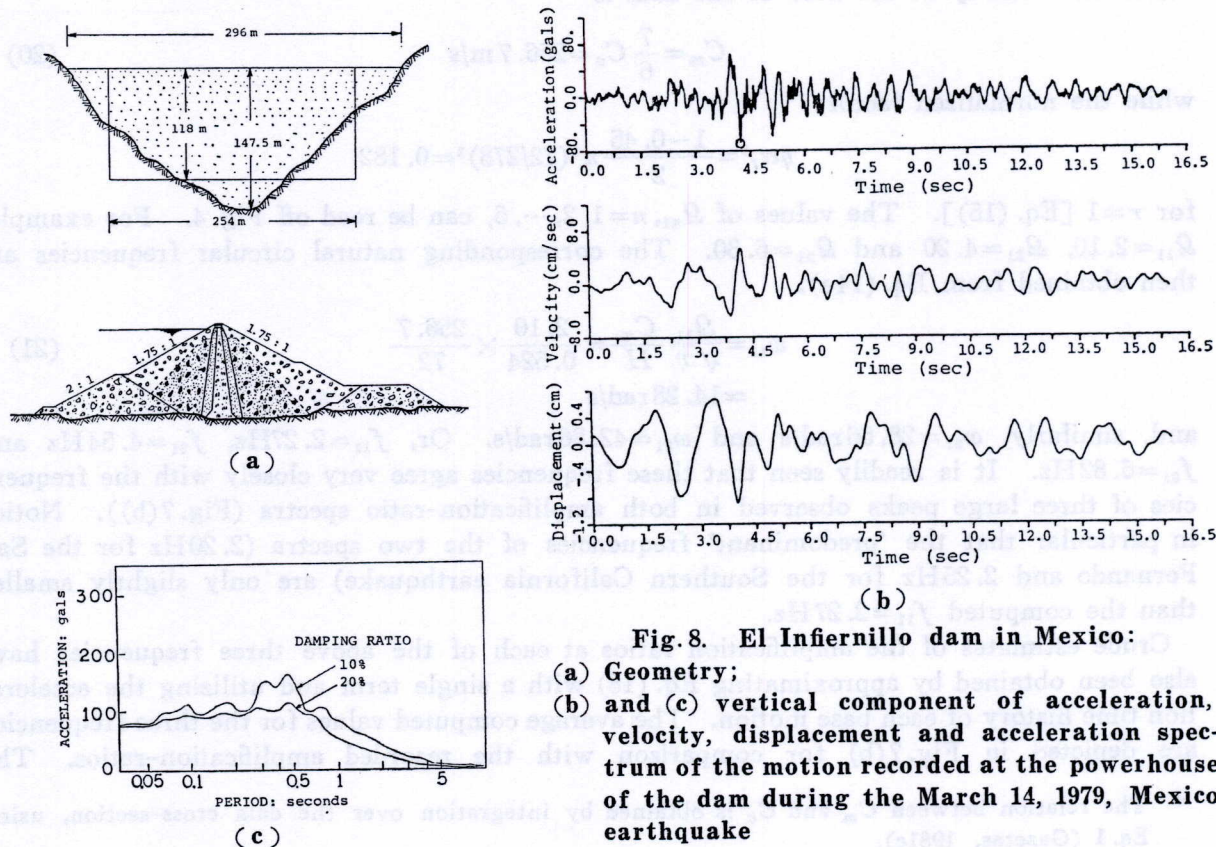
agreement is very reasonable, given the approximate nature of the computation, and reinforces the confidence in using the presented theory.

Infiernillo Rockfill Dam, Mexico

The maximum cross-section and the profile along the axis of this 147.5 m-high rockfill dam are shown in Fig. 8(a). As mentioned in the introduction the dam was recently shaken by a very strong earthquake at an epicentral distance of about 87 km. Motions were recorded in the underground powerhouse in rock near the base of the dam and on the crest of the dam. The maximum horizontal acceleration in the rock was about 130 gal the maximum acceleration at the crest was about 360 gal. In the vertical direction, the corresponding maximum values were 70 and 340 gals approximately. The residual crest settlement was about 12 cm and most of the movements took place in the upper 15 m of the dam, while most of the settlements occured in the upper 40 m. The reader is referred to the report by the Mexican Comisión Federal de Electricidad (1980) for a very detailed account of the performance of the dam during the aforementioned earthquake.

Fig. 1 and Fig. 8(b) display the vertical acceleration, velocity and displacement time histories obtained from the vertical components of the recorded motions at the crest and in the powerhouse while Fig. 8(c) shows the corresponding 10% and 20% damped response spectra. An "effective" value of 15% was selected as appropriate for the fundamental mode, for this level of shaking. Larger values were used for the higher modes.

On the basis of full-scale resonant tests by means of two eccentric load shakers an average shear wave velocity of about 480 m/s is deduced. This velocity apparently corresponds to very low shearing strain amplitude (of the order of 10^{-6} or less). To estimate a representative "effective" value of shear wave velocity consistent with the strong level of shaking observed during the March 14, 1979 earthquake, one can use published

(a)

(b)

(c)

Fig. 8. El Infiernillo dam in Mexico:
(a) Geometry;
(b) and (c) vertical component of acceleration, velocity, displacement and acceleration spectrum of the motion recorded at the powerhouse of the dam during the March 14, 1979, Mexico earthquake

empirical data relating soil shear modulus to shear strain amplitude (e.g., Makdisi & Seed, 1978; Mori, Ishihara et al., 1980). For an estimated "effective" strain amplitude of about 0.0005* the shear modulus reduces to about 1/2 of its low-strain-amplitude modulus (Makdisi & Seed, 1978). Thus, in our analysis we use

$$C_a \simeq 480 \sqrt{0.5} \simeq 340 \, \text{m/s}$$

Using the powerhouse motion as input in the analysis the maximum crest acceleration of the "equivalent" rectangular dam is computed equal to 415 gal which exceeds the recorded peak acceleration (334 gal) by about 24%. This 'prediction' should be considered as reasonably satisfactory given: (1) the approximate modeling (through an elastic "effective" modulus and damping ratio) of the truly nonlinear and inelastic soil behaviour during such a strong shaking; and (2) the very random nature of peak accelerations, which are always difficult to accurately predict.

Sannōkai Earth Dam, Japan

Okamoto et al. (1969) have reported a study of the behaviour of Sannōkai dam (Fig. 9) during several distant earthquakes, recorded on seismometers that had been installed at various locations on and inside the dam, as well as on the abutments. The dam is an earthfill embankment with a central impervious core, maximum height of 37 m and crest length of 145 m; (see Okamoto, 1973, for additional information).

Of interest here are the vertical components of motions recorded during two earthquakes with peak ground accelerations of 6 gal and 2.6 gal. The corresponding maximum crest accelerations were 19.5 gal and 7 gal, respectively. Amplification spectra of the two motions, computed by dividing Fourier amplitudes of acceleration of the crest records by those of the abutment records ('input' ground motion), are displayed in Fig. 10. Both spectra exhibit several well defined peaks that are believed to be the result of resonance
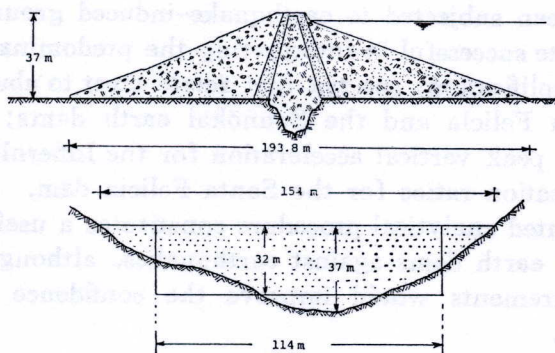
Fig. 9. **Geometry of Sannōkai dam in Japan**
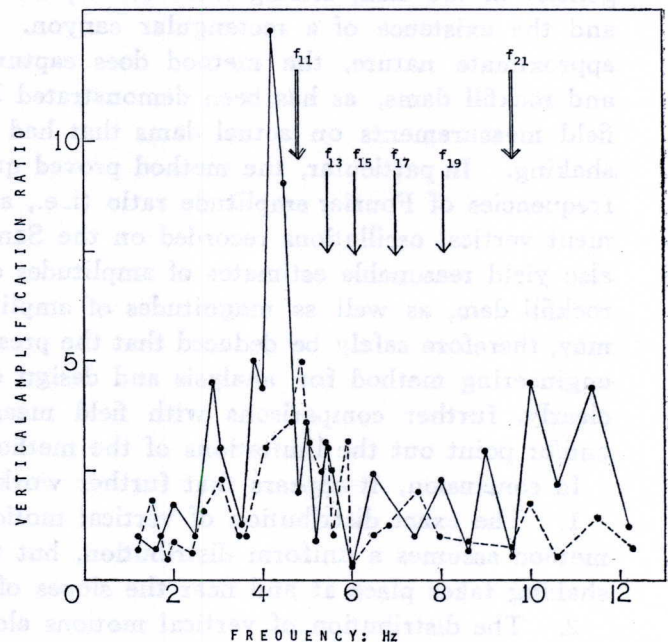
Fig. 10. **Crest-to-abutment amplification spectra from two earthquakes recorded on Sannōkai dam**

* Based on the statistical results of Gazetas, DebChaudury and Gasparini (1981) for lateral vibrations of earth dams.

phenomena; the frequencies at which they occur correspond to the natural frequencies of the dam in the vertical direction. The developed procedure is then used to independently predict the same frequencies.

Approximating the canyon geometry as indicated in Fig. 9, we have $H \simeq 32$m and $L \simeq$ 114m. Okamoto (1973) has backfigured the average shear wave velocity from the resonant frequencies observed in five upstream-downstream motions: $C_a \simeq 220$m/s -230m/s. Herein, we take $C_a = 225$m/s. In addition, Poisson's ratio is taken as $\nu = 0.35$. Thus, the first two fundamental frequencies are obtained as follows:

$$\eta \alpha_1{}^2 \simeq \frac{1-0.35}{2} \pi^2 \left(\frac{32}{114}\right)^2 \simeq 0.253$$

and, from Fig. 4, $\Omega_{11} \simeq 2.105$, $\Omega_{21} \simeq 4.208$. Eq. (14a) then leads to $f_{11} \simeq 4.80$Hz and $f_{21} \simeq 9.60$Hz. These two values (displayed with double-line arrows in Fig. 10) are in very satisfactory agreement with the two predominant frequencies of each recorded amplification spectrum.

The computed higher frequencies f_{13}, f_{15}, f_{17} and f_{19}, also depicted in Fig. 10 as single-line arrows, match reasonably well the frequencies of some secondary peaks of the two amplification spectra.

CONCLUSION

Vertical oscillations may adversely affect the liquefaction potential, slope stability and residual deformations of embankment dams and, thus, should be of concern to geotechnical-earthquake engineers.

The paper has presented a simple analytical method which considers both the inhomogeneity of the dam, arising from the dependence of soil stiffness on the confining pressure, and the existence of a rectangular canyon. Despite certain assumptions of simplifying approximate nature, the method does capture the key dynamic characteristics of earth and rockfill dams, as has been demonstrated by evaluating its predictions in the light of field measurements on actual dams that had been subjected to earthquake-induced ground shaking. In particular, the method proved quite successful in interpreting the predominant frequencies of Fourier amplitude ratio (i.e., amplification) spectra that relate crest to abutment vertical oscillations recorded on the Santa Felicia and the Sannōkai earth dams; it also yield reasonable estimates of amplitudes of peak vertical acceleration for the Infiernillo rockfill dam, as well as magnitudes of amplification ratios for the Santa Felicia dam. It may, therefore safely be deduced that the presented analytical procedure constitutes a useful engineering method for analysis and design of earth dams against earthquakes, although, clearly, further comparisons with field measurements would improve the confidence in and/or point out the limitations of the method.

In conclusion, it appears that further work should attempt to clarify:

1. The exact distribution of vertical motions across the width of a dam; the presented method assumes a uniform distribution, but there is little doubt that the strongest vertical shaking takes place at and near the slopes of the dam.

2. The distribution of vertical motions along the depth of the dam; since this distribution depends primarily on the variation of soil stiffness with depth from the crest, the presented theory is expected to be reasonably accurate, judging from the very satisfactory performance of an analogous theory for lateral and longitudinal vibrations of similarly inhomogeneous dams, presented recently by the author (Gazetas, 1981 a b; Gazetas & Abdel-Ghaffar, 1981)

3. The significance of 3-dimensional effects, especially in dams built in narrow and

v-shaped canyons; at present, there is little published information on the basis of which to estimate the possible error in assuming an "equivalent" rectangular canyon.

4.   The actual size of tensile strains induced near the slopes and the crest of a dam during vertical vibrations; it should be emphasized, incidentally, that a crucial (albeit implicit) assumption of the method (as well as of any elastic method) is that the developing tensile strains are, to a great extent, compensated by the compressive strains due to the self weight of the dam-an assumption that may be unrealistic for the soil immediately below the crest, during strong shaking.

5.   The influence of inelastic soil behaviour on response to strong earthquakes that cause shearing deformations.

Until these questions are fully answered, the presented simple but logical method can serve as a useful tool, guiding the seismic design of embankment dams and helping evaluate their earthquake performance.

NOTATION

A', A''=integration amplitude constants in Eqs. (9) and (13), taken equal to unity in the subsequent analysis

α_r=dimensionless factor given by Eq. (15)

B=width of the base of the dam (Fig. 3)

$\Gamma_{nr}=(n, r)$ mode participation factor (Eq. 19)

C=shear wave velocity$=\sqrt{G/\rho}$

$E_{nr}=0.25\,r\pi\,\Gamma_{nr}$ [Eq. (19) and Fig. 6]

E=Young's modulus of the material of the dam

f_{nr}=natural frequency of vibration in the (n, r) mode

G=shear modulus of the material of the dam

H=height of the dam (Fig. 3)

η=dimensionless factor, function of Poisson's ratio (Eq. 4c)

L=length of the dam (Fig. 3)

$M_{nr}(z)=(n, r)$ th modal vertical displacement shape in the vertical direction [Eq. (13) and Fig. 5]

$N_r(x)=r$ th modal vertical displacement shape in the longitudinal direction [Eq. (9)]

ν=Poisson's ratio

$v(x, z; t)$=vertical displacement, function of x, z and time

$V_{nr}=M_{nr}N_r=(n, r)$ th modal vertical displacement shape

σ_z=vertical normal stress (Fig. 3)

τ_{xz}=vertical shear stress (Fig. 3)

$\omega_{nr}=2\pi\,f_{nr}$=natural circular frequency (in rad/s) of the (n, r) mode

Ω_{nr}=dimensionless frequency factor given graphically in Fig. 4, related to ω_{nr} through Eq. (14 a)

Subscripts

m : denotes soil parameters at the base of the dam

a : denotes spatially average values of soil parameters throughout the dam

REFERENCES

1)   Abdel-Ghaffar, A. M. and Scott, R. F. (1978) : "An investigation of the dynamic characteristics of an earth dam," Earthq. Engrg. Res. Lab. Report EERL 78-02, Calif. Inst. of Tech., Pasadena.

2)   Abdel-Ghaffar, A. M. and Koh, A-S. (1981) : "Longitudinal vibration of nonhomogeneous earth dams," Int. J. of Earthq. Engrg. & Str. Dyn., Vol. 9, No. 4.

3)   Ambraseys, N. N. (1960) : "On the shear response of a two-dimensional truncated wedge subjected to an arbitrary disturbance," Bull. of the Seisnological Soc. of Am., Vol. 50, pp. 45-46.

4) Chopra, A. K. (1967) : "Earthquake response of earth dams" J. Soil Mech. Found. Engrg. Div. ASCE, Vol. 93, SM 2.

5) Comision Federal de Electricidad (1980) : "Performance of El Infiernillo and La Villita Dams including the earthquake of March 14, 1979," CFE Report No. 15, Mexico.

6) Gazetas, G. (1981 a) : "A new dynamic model for earth dams evaluated through case histories," Soils and Foundations, Vol. 21, No. 1, pp. 67-78.

7) Gazetas, G. (1981 b) : "Longitudinal vibrations of embankment dams," J. Géotech. Engrg. Div. ASCE, Vol. 107, GT 1, pp. 21-40.

8) Gazetas, G. (1981 c) : "Shear vibrations of vertically inhomogeneous earth dams," Int. J. Num. Anal. Meth. Geomech. (in press).

9) Gazetas, G. and Abdel-Ghaffar, A. M. (1981) : "Earth dam characteristics from full-scale vibrations," Proc. X Int. Conf. Soil Mech. & Found. Engrg., Stockholm, Sweden, Vol. 3, No. 1017, pp. 207-210.

10) Gazetas, G., DebChaudhury, A. and Gasparini, D. (1981) : "Random vibration analysis for the seismic response of earth dams," Géotechnique, Vol. 31, No. 2, pp. 261-277.

11) Hatanaka, M. (1955) : "Fundamental considerations on the earthquake resistant properties of the earth dam," Bull. No. 11, Disast. Prev. Res. Inst., Kyoto Univ.

12) Ishizaki, H. and Hatakeyama, N. (1962) : "Consideration on the dynamical behaviors of earth dams," Bull. 52, Disast. Prev. Res. Inst., Kyoto Univ.

13) Makdisi, F. I. and Seed, H. B. (1978) : "Simplified procedure for estimating dam and embankment earthquake-induced deformations," J. Geotech Engrg. Div. ASCE, Vol. 104, GT 7, pp. 849-867.

14) Minami, I. (1969) : "On vibration characteristics of fill dams in earthquakes," Proc. 4 th World Conf. Earthq. Engrg., Santiago, Chile, paper A-5, pp. 101-115.

15) Mori, K., Ishihara, K., Takeya, K. and Kanazashi, K. (1980) : "Seismic stability analysis of Kokubo dam," Proc. Conf. on Design of Dams to Resist Earthq., Inst. Civ. Engrs, London, pp. 83-90.

16) Okamoto, S., Hakuno, M., Kato, K. and Kawakami, F. (1969) : "On the dynamical behaviour of an earth dam during earthquakes," Proc. 4 th World Conf. Earthq. Engrg., Santiago, Chile.

17) Okamoto, S. (1973) : "Introduction to Earthquake Engineering" J. Wiley and Sons, New York, Chap. 15., "Earthquake Resistance of Embankment Dams."

18) Richart, F. E. and Wylie, E. B. (1977) : "Influence of dynamic soil properties on response of soil masses," Struct. & Geotech. Mech., Prentice-Hall, pp. 141-162.

19) Seed, H. B. (1979) : "Considerations of earthquake resistance of earth and rockfill dams," Géotechnique, Vol. 29, No. 3, pp. 15-63.